

Formation of Macrocyclic Poly(oxymethylene) with Narrow Molecular Weight Distribution on the Lamellar Crystals

Masaki Hasegawa,^{*,†} Kaoru Yamamoto,[‡] Toshio Shiwaku,[‡] and Takeji Hashimoto[§]

Department of Synthetic Chemistry, Faculty of Engineering, The University of Tokyo, Hongo, Bunkyo-ku, Tokyo 113, Japan, Polyplastics Co. Ltd., Research Center, 973 Miyajima, Fuji, Shizuoka 416, Japan, and Department of Polymer Chemistry, Faculty of Engineering, Kyoto University, Sakyo-ku, Kyoto 606, Japan

Received September 12, 1989; Revised Manuscript Received November 15, 1989

ABSTRACT: Poly(oxymethylene) (POM) with a narrow molecular weight distribution was isolated by alkaline degradation of the bulk polymer, which was derived from 1,3,5-trioxane (TOX) under various cationic polymerization conditions. The isolated POM had no end groups (confirmed by ¹H NMR spectroscopic analysis) and was stable to both heat and alkali conditions, compared to ordinary POM. On the basis of these observations, it was concluded that the isolated POM had a macrocyclic structure. The number-average molecular weight of cyclic POM was in the 1300–2300 range, having a ratio of 1.1–1.2 (\bar{M}_w/\bar{M}_n). The molecular weight of the cyclic POM increased with an increase in the thickness of the crystal lamellae of the original POM, and the calculated length of the cyclic POM was nearly equal to twice the thickness of the original POM crystal lamellae. These facts have been interpreted as meaning that the size of cyclic POM is determined by the lamellar thickness and that a macrocycle is formed by an intramolecular transacetalization on the surface of the crystal lamella. Cyclic POM underwent a further polyaddition reaction in the crystalline state upon the γ -ray irradiation.

Introduction

It is well-established that a linear high molecular weight poly(oxymethylene) is obtained with a certain amount of cyclic oligomers by the cationic polymerization of cyclic acetals, such as 1,3,5-trioxane (TOX) and 1,3-dioxolane.^{1–3} These cyclic products can be formed by the intramolecular transacetalization of a linear cation^{2,4} or by the ring expansion of a cyclic cation.^{5,6} The former reaction, a so-called "back-biting" reaction, forms two species: a shorter linear polymer with an active cationic end group and thermodynamically stable small membered rings (e.g. a six- or eight-membered ring). The back-biting reaction has seriously influenced the reaction rate during the initial stage of the polymerization of TOX. This is because the polymerization is greatly accelerated by highly active cyclic byproducts, such as tetraoxane. These cyclic byproducts (detected in appreciable quantities in the initial stage) are formed only by a back-biting reaction. This fact indicates that the polymer grows through linear active intermediates (such as an oxycarbenium ion) at least in a certain step of the chain propagation.

Regarding the solution polymerization of TOX catalyzed by BF₃·OEt₂, Okamura et al.^{7,8} have reported that the amount of tetraoxane was almost constant during the induction period because of the equilibrium between formation and consumption. After the induction period, the amount of tetraoxane decreased owing to the reduced back-biting reaction, which was caused by the restricted mobility of the cationic chain end. The propagation reaction is considered to proceed on the deposited crystal surface while tetraoxane and TOX are consumed under a heterogeneous reaction system. Thus, the whole behavior during the polymerization reaction of TOX must be closely related to the crystallization of the growing polymer.

The polymerization of TOX is a typical example for simultaneous polymerization and crystallization, since the

polymer is insoluble and crystallizes at a high rate in conventional solvents for cationic polymerization. The Freiburg group proposed the building step of the crystal, taking into account each chemical step in the polymerization of TOX.^{9,10} They assumed that the low-molecular-weight "tail", which was observed within the molecular weight range $(1-3) \times 10^3$ on a gel permeation chromatographic (GPC) curve of TOX-propylene oxide copolymers, was a mixture of macrocycles produced by a back-biting reaction on the crystal.¹¹ However, there was no evidence for the formation of macrocycles, except that the "tail" had a low molecular weight in comparison with the linear polymer portion. On the other hand, Jaacks reported the formation of an alkaline-stable polymer with an average molecular weight of 10^3 as part of poly(oxymethylene) (POM) obtained by the homopolymerization of TOX in a cyclohexane solution.¹² He found that this alkaline-stable portion did not contain a methoxy end group (using the Zeisel method) and assumed that this portion (ca. 10 wt %) had a macrocyclic structure resulting from a back-biting reaction. The cyclic byproduct, however, usually had a small ring, and in the case of the polymerization of TOX, six- (i.e. reproduced monomer) and eight-membered (tetraoxane) rings were produced as the main cyclic byproducts accompanied by very small amounts of 10- and 12-membered rings, which were only detectable by gas chromatography.² Thus, it does not explain why the molecular weight of the alkaline-stable portion was not small but around 10^3 .

The polymerization of TOX progressed under a heterogeneous system between a deposited crystal and a monomer solution (or melt). Thus, the reactions occurred on the solid-to-liquid interfaces. Such an interesting interplay between the chemical reaction and the physical process motivated our present studies. First of all, we examined the cationic bulk, suspension, and solution polymerizations of TOX and confirmed that these polymerizations always gave a considerable amount of low-molecular-weight byproduct (ca. 15 wt %), which was stable to heat and to alkali conditions, accompanied by high-molecular-

^{*} The University of Tokyo.

[†] Polyplastics Co. Ltd.

[§] Kyoto University.

Table I
Polymerization Conditions of 1,3,5-Trioxane and Amounts of the Alkaline-Stable Portion and the Low-Molecular-Weight Portion

sample code	cat. ^a (10 ⁻⁶ mol)	quench time, min	conversn, %	\bar{M}_w	alkaline-stable portion, %	portion of the low-molecular-weight peak, ^b %
S-1	BF ₃ ·OBU ₂ (9.6)	3	78	56 600	13	17
S-2	CF ₃ SO ₃ H (0.15)	7	50	70 500	15	21
S-3	Et ₃ OPF ₆ (8.1)	13	65	58 100	13	25

^a Catalyst was added to 20.0 g (0.222 mol) of 1,3,5-trioxane at 70 °C. ^b Calculated from the portion above the break line in Figure 1a.

weight homo-POM. In this paper we report on the primary structure and molecular weight distribution of the alkaline-stable POM and discuss the formation mechanism by taking into account the effect of crystallization during polymerization.

Experimental Section

Materials. 1,3,5-Trioxane (TOX), boron trifluoride-dibutyl etherate (BF₃·OBU₂), 1,1,1,3,3,3-hexafluoro-2-propanol (HFIP), and 1,2-dichloroethane (EDC) were purified by distillation before use. TOX contained 400 ppm of trioxepane and 45 ppm of water as impurities after purification by distillation, as determined by gas chromatography and the electrochemical Karl-Fischer technique, respectively. Trioxepane results in an oxyethylene unit in the polymer main chain and/or a hydroxyethyl end group, which is stable to alkaline degradation.

Measurements. GPC Analysis. GPC was carried out with a Tosoh HPLC-8020 using HFIP as an eluent monitored by the refractive index. The calibration curve for the molecular weight against the elution time was determined by the low-angle laser light scattering method with a Tosoh LS-8000 for molecular weights above 10⁴ and by the reduced molecular weight method for molecular weights under 10⁴ using monodispersed poly(tetrahydrofuran) samples. The calibration curve determined by both methods became a smooth master curve within the 10³–10⁶ region of molecular weight. The number-average molecular weight (\bar{M}_n), weight-average molecular weight (\bar{M}_w), and polydispersity (PD = \bar{M}_w/\bar{M}_n) were calculated from this standard curve.

¹H NMR. ¹H NMR in a HFIP-*d*₂ solution was measured with a Bruker AM-300 instrument (300-MHz FT-NMR) using tetramethylsilane as an internal standard at 25 °C.

Small-Angle X-ray Scattering (SAXS). In order to estimate the thickness of POM crystal lamellae, the long period of POM was measured by the SAXS apparatus with a Rigaku rotating-anode generator (Cu K α , 50 kV \times 200 mA), a position sensitive proportional counter, and an optical system (described elsewhere¹³). The SAXS profiles were corrected for both slit-height and slit-width smearing effects as well as background scattering due to thermal diffuse scattering. The long period was determined from the desmeared profiles corrected for the Lorentz factor.

Thermal Analysis. The thermal behavior of POM was studied on the basis of differential scanning calorimetry (DSC) and thermogravimetry (TGA) under a dry-nitrogen atmosphere using a Perkin-Elmer TAS-7 system.

Polymerization and Alkaline Degradation. The typical procedure for the preparation of POM from TOX is as follows:

(1) **Bulk Polymerization.** To molten bulk TOX (20.0 g, 0.222 mol), was added 9.6×10^{-7} to 9.6×10^{-6} mol of BF₃·OBU₂ in cyclohexane (0.71 wt % solution) at 70–110 °C under a dry-nitrogen atmosphere. After an induction period for a few seconds, TOX became turbid and then changed into a white solid. After 3–13 min, water containing 750 ppm of triethylamine (10 mL) was added to the reaction mixture. When the mixture was cooled to 0 °C, the resulting white solid was crushed, pulverized, and washed repeatedly with warm water (60 °C) and acetone to remove any unreacted monomer and oligomer.

(2) **Suspension Polymerization.** To TOX (23.4 g, 0.260 mol) suspended in liquid paraffin (50 mL) was added 4.8×10^{-6} mol of BF₃·OBU₂ in cyclohexane (0.71 wt % solution) at 70–90 °C under a dry-nitrogen atmosphere. After 10 min, the reaction mixture was quenched in the same way as during the bulk polymerization. White grains were separated from the liquid

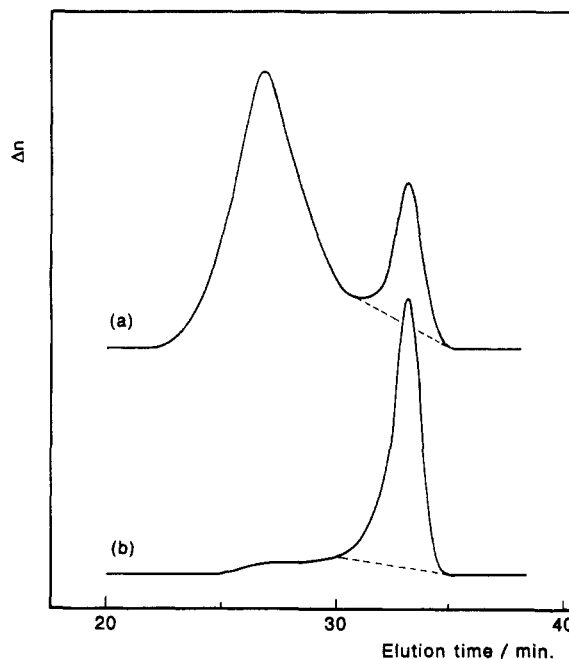


Figure 1. GPC curves of POM: (a) POM obtained by bulk polymerization of TOX (S-3) and (b) its alkaline-stable portion (S-3R). For the polymerization conditions and molecular weight, see Tables I and II.

paraffin by filtration and washed well with toluene and acetone.

(3) **Solution Polymerization.** To a solution of TOX (11.2 g, 0.124 mol) in EDC (50% solution by volume) was added 1.49×10^{-7} mol of CF₃SO₃H in cyclohexane (0.36 wt % solution) at 32 °C under a dry-nitrogen atmosphere. The mixture was stirred for 30 min, and the reaction was quenched with triethylamine. The precipitates were collected by filtration and washed well with methanol and acetone.

(4) **γ -Ray-Induced Solid-State Polymerization.** The polymerization was carried out by using ⁶⁰Co γ -ray. Irradiation was performed with crystalline TOX under a dry-nitrogen atmosphere at 30 °C with 1×10^4 Gy.

(5) **Alkaline Degradation of POM.** POM was treated with 4.2×10^{-2} M ammonia solution in water/methanol (40/60; 80 mL) for 1 h at 170 °C in an autoclave and then reprecipitated from HFIP/acetone.

Results and Discussion

Structure of the Lower Molecular Weight POM. The conditions for the bulk polymerization of TOX using three kinds of catalysts (i.e. initiators) and the amounts of alkaline-stable portion are listed in Table I. The typical GPC curve (Figure 1a) of POM, obtained by bulk polymerization, showed a characteristic bimodal distribution without a solvent peak. Similar GPC analyses of POM had been carried out by Ito et al.¹⁴ and the Freiburg group¹¹ for the copolymer of TOX with ethylene oxide or propylene oxide using *N,N*-dimethylformamide as an eluent at 140 °C. However, regarding their GPC curves, no noticeable peaks (except for the main peak) have been

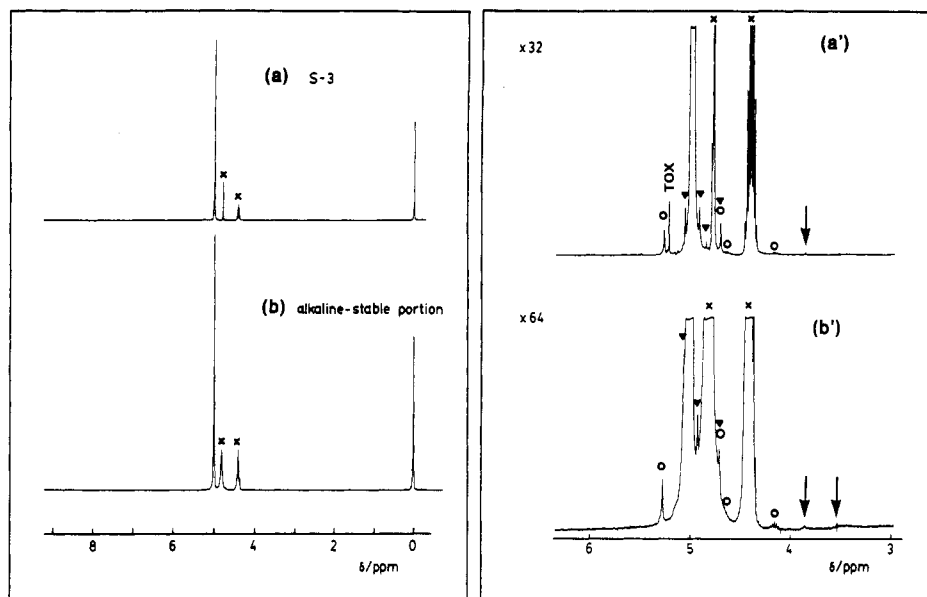


Figure 2. ^1H NMR spectra of (a) POM S-3 and (b) its alkaline-stable portion, S-3R. In each magnified spectra: (a') $\times 32$; (b') $\times 64$; (O) ^{13}C satellite, (∇) side spinning band, and (\times) solvent peaks. A singlet at δ 5.20 in (a') corresponds to a residual monomer; for other assignments, see text and ref 23.

Table II
Molecular Weight of POM before (S-3, Figure 1a) and after Alkaline Degradation (S-3R, Figure 1b)

sample	entire polymer ^a			portion of the low-molecular-weight peak ^b		
	\bar{M}_n	\bar{M}_w	\bar{M}_w/\bar{M}_n	\bar{M}_n	\bar{M}_w	\bar{M}_w/\bar{M}_n
S-3	6430	58100	9.05	1500	1670	1.12
S-3R	1930	5950	3.08	1680	2070	1.24

^{a,b} Calculated from (a) the entire portion eluted from 22 to 35 min and (b) the portion above the break line in parts a and b of Figure 1, respectively.

seen in the low-molecular-weight region other than the "tail".¹¹ The difference between their results and ours with GPC analysis would come from a difference in the eluent used. As shown in Figure 1b, after alkaline degradation, only a narrow distribution peak was observed, of which the elution time exactly corresponded to that of the lower molecular weight portion in its original POM. The molecular weights of POM before and after alkaline degradation are listed in Table II. Moreover, the amount of the alkaline-stable portion was nearly equal to or slightly less than that of the lower molecular weight peak of the original POM (Table I). These results indicate that the majority of the alkaline-stable portion exists in the lower molecular weight portion of its original POM.

Some side reactions can proceed during the chain propagation, such as a chain transfer to contaminated H_2O (Scheme 1a) and to a methylene group in a polymer chain (Scheme 1b), as well as transacetalization to an oxygen in a polymer chain (Scheme 1c). The attack of an oxycarbenium ion on an intramolecular oxygen results in the formation of another carbenium end group and a cyclic oligomer or polymer (Scheme 1d, back-biting reaction). In the bulk polymerization of TOX catalyzed by $\text{BF}_3\cdot\text{OEt}_2$ in the presence of water, the initiation reaction forms the hydroxyl end group.¹⁵ When all of these reactions occur, seven kinds of POM can be formed with various end groups, as shown in Scheme II. POM with either a hydroxyl or a formyl end group is unstable to heat annealing and/or alkaline degradation, and such treatments result in the depolymerization of POM from the chain ends. Therefore, POM 1–5 in Scheme II are unable to exist after heat annealing and alkaline degradation, whereas

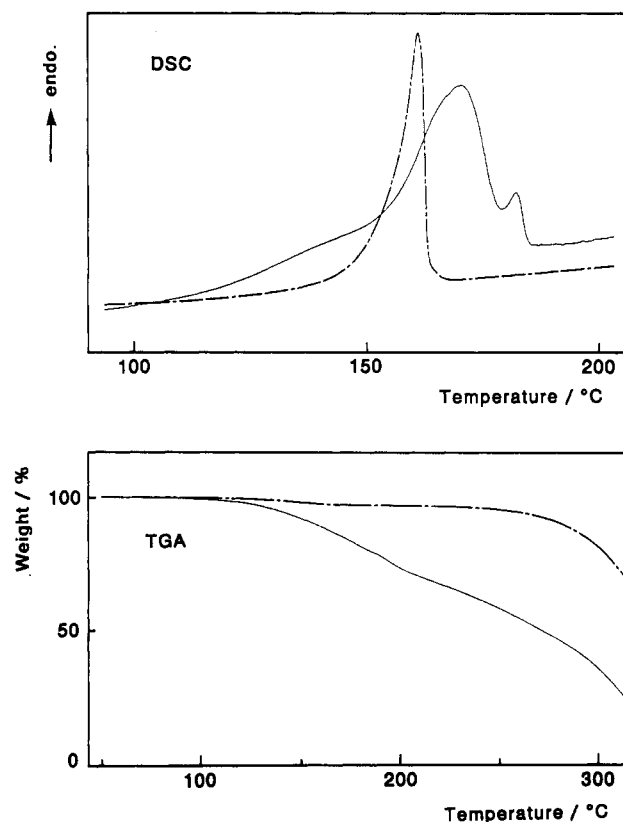
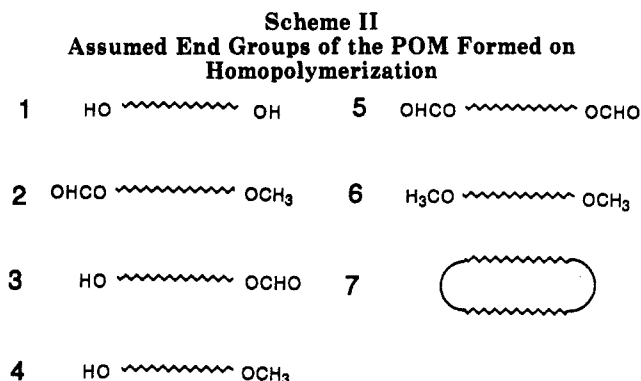
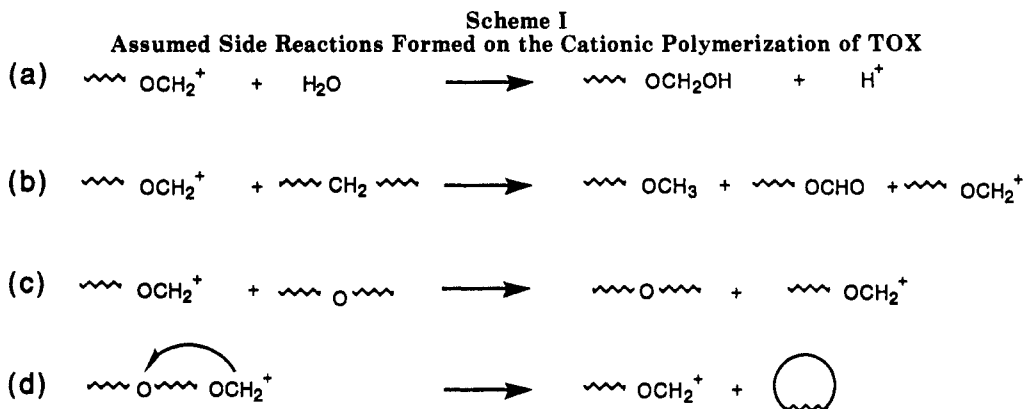


Figure 3. DSC and TGA analyses of original POM (S-3) (—) and alkaline-stable portion (S-3R) (---). Heating rate of $10^\circ\text{C}\cdot\text{min}^{-1}$.

POM 6 and 7 are stable. Then, the alkaline-stable portion probably consists of POM with two methoxy end groups and/or with no end group (i.e. a cyclic polymer).

To elucidate the structure of the alkaline-stable polymer, ^1H NMR and thermal analysis were carried out.

The ^1H NMR spectrum (Figure 2a,a') of the original POM S-3 showed no distinct signal, except for a singlet at δ 4.99, which corresponds to the oxymethylene unit in a polymer main chain because of its high molecular weight. In the ^1H NMR spectrum (Figure 2b,b') of POM S-3R (the alkaline-stable portion of S-3), other than the sig-



nal of the oxymethylene unit at δ 4.99, only two small singlets were observed at δ 3.85 and 3.52. These peaks could be assigned to the protons of the oxyethylene unit caused by trioxepane contaminated in TOX and to the protons of the methoxy end group. If S-3R has two methoxyl end groups (namely, the structure of S-3R is 6), the methoxy signal must show 4.8% of the oxymethylene signal in intensity on the basis of the molecular weight of S-3R ($\bar{M}_n = 1930$) calculated from GPC. However, the methoxy signal intensity was actually very weak, compared with the ^{13}C satellite signal of the oxymethylene unit (0.5% in intensity). These results indicate that the alkaline-stable portion has much fewer methoxyl end groups and that its structure is mainly cyclic.

In the DSC curves, the crystal melting point of the alkaline-stable portion was lower, but sharper, than that of the original POM (Figure 3a). The observed differences in the melting behavior are attributed to the lower molecular weight and the smaller PD of S-3R compared to the original POM S-3. The thermal stability of S-3R was enhanced remarkably, compared to that of S-3, as can be seen in the TGA curves (Figure 3b). Under a dry-nitrogen atmosphere, S-3 began to lose its weight at about 100 °C, while S-3R was entirely stable up to about 230 °C. The difference in the TGA curves can be explained by the absence or the presence of hydroxyl and formyl end groups for S-3R and for S-3. Therefore, the hydroxyl or formyl end groups rarely exist in S-3R.

Figure 4 shows the GPC curves of the products after γ -ray irradiation of S-3R at 115 °C (insorce) or at -78 °C (and postannealing at 145 °C). In both cases of insorce and post polymerization at a temperature slightly below the melting point of S-3R (mp 161 °C, determined from the peak temperature of endothermic curve on DSC in Figure 3a), the elution time of the GPC main peak was exactly the same as that of nonirradiated S-3R, whereas a new peak for the higher molecular weight portion appeared. The new peak is regarded as resulting from the products formed by a crystalline state reaction of the

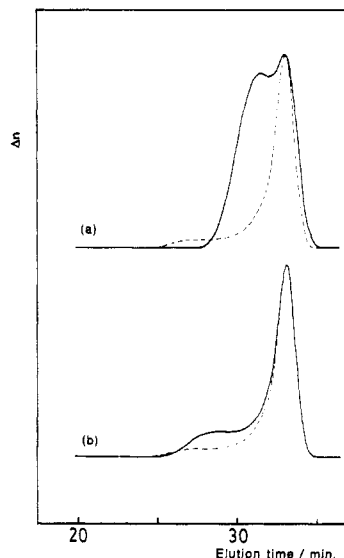


Figure 4. GPC curves of alkaline-stable POM after γ -ray irradiation: (a) irradiated with 18.5 Mrad at -78 °C, followed by isothermal annealing at 145 °C for 20 h, $\bar{M}_n = 3260$; (b) irradiated with 2.5 Mrad at 115 °C, $\bar{M}_n = 2790$. The broken line shows nonirradiated polymer (S-3R), $\bar{M}_n = 1930$.

cyclic POM upon γ -ray irradiation. If we assume that a linear polymer underwent an addition reaction, the chain of a reacting polymer is statistically cleaved in half; then, the addition reaction progresses. As a result, the \bar{M}_n should not change upon γ -ray irradiation, unless both scission and termination occur in the linear polymer chain. On the basis of the behavior of S-3R for γ -ray irradiation, it is also observed that the alkaline-stable portion consists of cyclic POM. The increase in the high molecular weight portion would result from a ring-opening polyaddition reaction of cyclic POM in the crystalline state, which is similar to the reaction observed for the solid-state polymerization of TOX.

In conclusion, (i) POM prepared by the cationic polymerization of TOX gives a bimodal molecular weight distribution, (ii) the low molecular weight portion can be isolated by the alkaline degradation of the as prepared homo-POM, and (iii) the alkaline-stable portion has a macrocyclic structure with an \bar{M}_n of ca. 2000 with a narrow molecular weight distribution (PD = 1.1~1.2).

Mechanism for the Formation of Macrocyclic POM with a Narrow Molecular Weight Distribution. The bimodal molecular weight distributions of POM was observed for the cationic bulk, solution, and suspension polymerizations, independent of our experimental conditions such as type and amount of the catalysts and reaction temperature. The quantity of the low molecular weight portion, however, changed according to the indi-

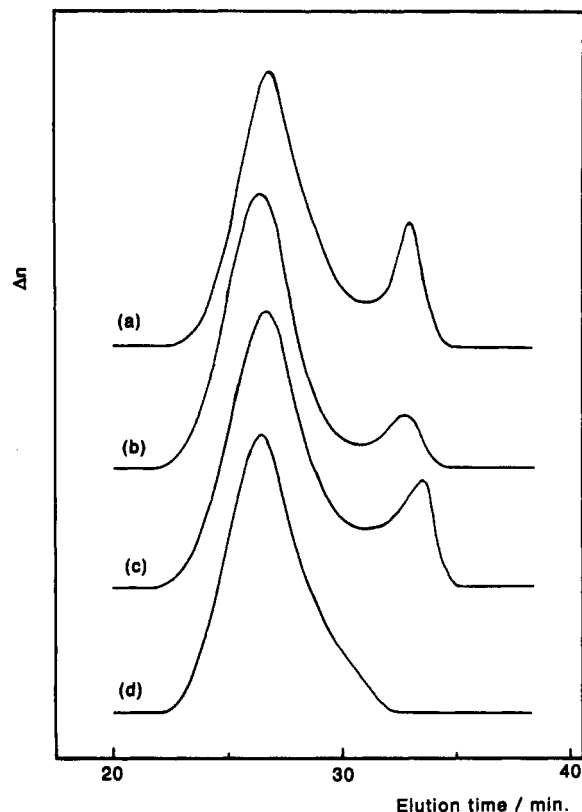


Figure 5. GPC curves of POM obtained by various polymerizations: (a) bulk polymerization at 70 °C catalyzed by $\text{BF}_3 \cdot \text{O}(\text{C}_2\text{H}_5)_2$, $\bar{M}_w = 55\,600$, for polymerization conditions see Table I (S-1); (b) suspension polymerization at 70 °C catalyzed by $\text{BF}_3 \cdot \text{O}(\text{C}_2\text{H}_5)_2$, $\bar{M}_w = 64\,200$; (c) solution polymerization at 32 °C catalyzed by $\text{CF}_3\text{SO}_3\text{H}$, $\bar{M}_w = 68\,600$; (d) γ -ray-induced solid-state polymerization at 30 °C, $\bar{M}_w = 98\,000$. For polymerization conditions of (b)–(d) see the Experimental Section.

vidual conditions. Under certain conditions, especially when the entire average molecular weight was low, the low molecular weight portion was inconspicuous or even unnoticeable. The relation between the quantity of the low molecular weight portion and the reaction conditions is not clear, though the retention time of this portion on GPC was reproducible during repeated runs. The typical GPC curves (Figure 5a–c) of the samples, obtained by bulk, suspension, and solution polymerizations of TOX, shows bimodal distribution, namely, the formation of both linear and cyclic polymers.¹⁶ In these polymerizations, POM crystals were always deposited from homogeneous TOX or from its solution during the course of polymerization. In contrast, the solid-state polymerization upon γ -ray irradiation gave POM with a unimodal distribution (Figure 5d). In this case, ring-opening polyaddition occurred along a certain axis of the monomer crystal and formed an extended chain crystal of POM.¹⁷ Consequently, the bimodal distribution could be observed only when lamellar crystals were simultaneously deposited during polymerization; i.e., the formation of cyclic POM seems to be influenced by lamellar crystals. Moreover, the peak elution time of the low molecular weight fraction (the molecular weight of the macrocycles) is almost independent of that of the high molecular weight linear POM, prepared under various conditions, as shown in Figures 6 and 7. The results suggest that a back-biting reaction, which forms a cyclic oligomer and/or polymer, does not occur at random but in a specific manner.

The cyclic POM may be formed by a back-biting reaction on the interface of POM lamellar crystals during a chain propagation reaction or during rearrangement into

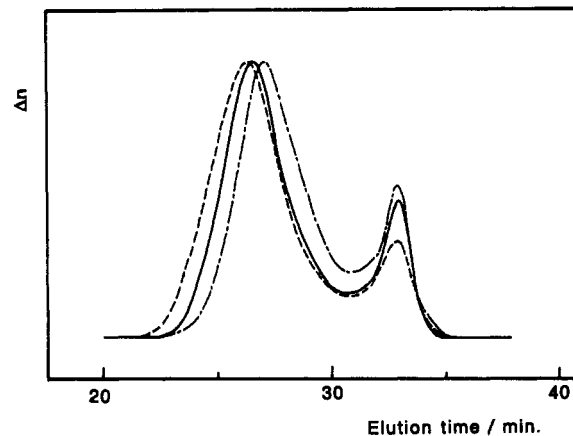


Figure 6. GPC curves of POM obtained by bulk polymerization catalyzed by $\text{BF}_3 \cdot \text{O}(\text{C}_2\text{H}_5)_2$: (---) polymerized at 70 °C, 2.2×10^{-6} mol of catalyst, $\bar{M}_w = 88\,800$; (—) at 70 °C, 9.6×10^{-7} mol of catalyst, $\bar{M}_w = 64\,600$; (---) at 100 °C, 9.6×10^{-6} mol of catalyst, $\bar{M}_w = 46\,500$.

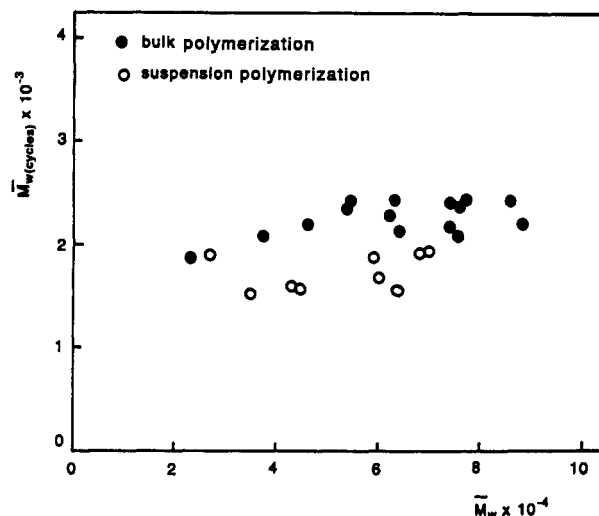
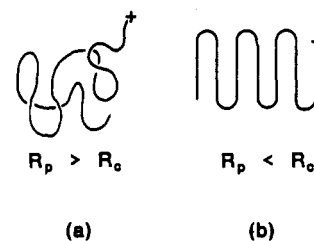


Figure 7. \bar{M}_w of the entire polymer versus \bar{M}_w of the macrocyclic polymer. \bar{M}_w of macrocycle was estimated by the low-molecular weight portion on each GPC curve.

Scheme III
Circumstances of Active Cationic Ends Dependent on the Relative Ratio of the Rate of Crystallization (R_c) to the Rate of Chain Propagation (R_p)^a

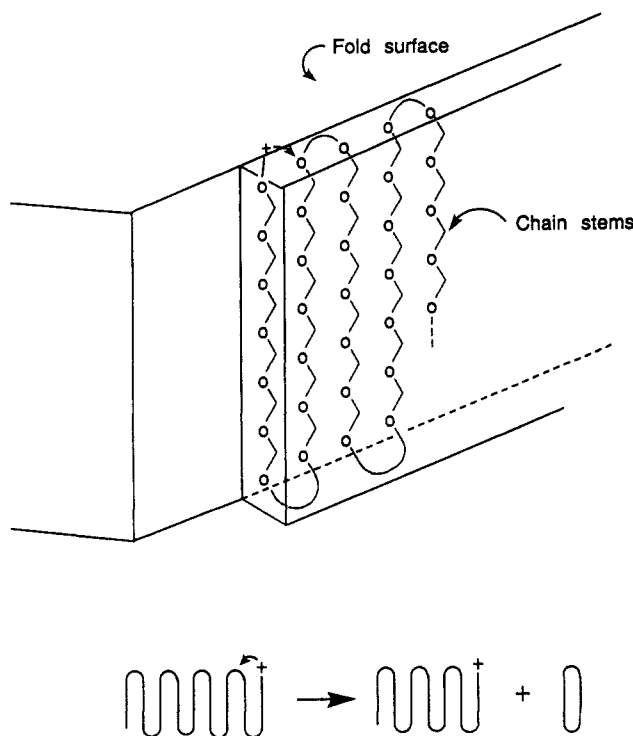


^a An active end is located on the deposited crystal when R_c is fairly larger than R_p , as shown in (b).

ordered lamellar crystals from small irregular crystals through the monomer–polymer chemical equilibrium.¹⁸

When R_p (the rate of chain propagation) is smaller than R_c (the rate of crystallization), active end groups may exist on a lamellar crystal with high probability (Scheme IIIb).¹⁹ An active cation in a lamellar crystal would be located near the oxygen in a polymer chain, which becomes a target for transacetalization. On the other hand, an active cation in a random coil (Scheme IIIa) is solvated and surrounded by the solvent and/or residual monomer. Namely, the cation on a lamellar crystal exists in a

Scheme IV
Schematic Representation of the Formation of Cyclic
POM: Diagram of the Cross Section on a Lamellar
Crystal Including an Active End
 POM crystal lamella



surrounding medium with a relatively high concentration of polymer oxygen and attacks a polymer oxygen (in the nearest stem of lamella) with a relatively high probability in comparison with a cation in a random coil. Moreover, under low monomer concentration conditions (e.g. the later stage of polymerization), the active cation would easily attack a polymer oxygen with a relatively high possibility than that in a monomer, owing to the small R_p .

In the case of transacetalization in crystal lamellae, the attack of the cationic end group on a polymer oxygen is considered to occur mainly on the surface of the crystal lamellae. Since a reaction on the surface is considered to be more probable than a reaction in the lamellar core (from a viewpoint of both the positional fluctuation of active sites and the reactivity and probability of the target oxygen). Both sites of the active cationic end group and the target oxygen in a polymer chain have a larger positional fluctuation when they exist on the surface of crystal lamellae than in the lamellar core. The larger positional fluctuation, in turn, results in a higher probability for a reaction on the surface. Moreover, the core oxygen has less reactivity for transacetalization because of a greater stabilization for the crystal lattice energy, which also results in an enhanced reaction probability on the lamellar surface. As another possible mechanism, the cationic species in the reaction system may attack the oxygen on the surface of a deposited crystal lamellar. In contrast, the oxygen in a lamellar core may not be attacked by an outside cation. For this mechanism, the active end groups form on the lamellar surfaces of deposited crystals.

If the active end group attacks an intramolecular polymer oxygen on the surface of a lamellar crystal through any mechanism, a cyclic polymer would be produced, and its length would be equal to twice the lamellar thickness

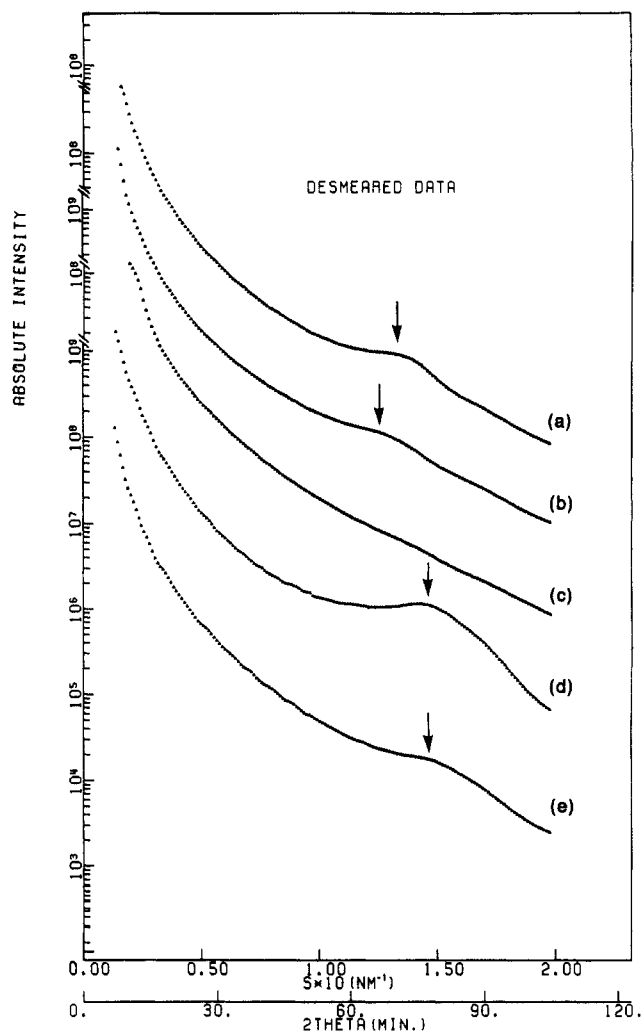


Figure 8. SAXS profiles from various POM specimens: (a) as-polymerized POM obtained by quenching bulk polymerization without washing; (b) the POM specimen of (a) subjected to isothermal annealing at 100 °C for 30 min and then measured at 100 °C for 3 h; (c) specimen of (a) subjected to washing to remove the residual monomer with warm water and acetone and drying under vacuum at 40 °C for 6 h [a corresponding GPC curve is shown in Figure 6 (—)]; (d) as-polymerized POM obtained by quenching suspension polymerization without washing; (e) specimen of (d) subjected to washing with toluene and acetone and drying under vacuum at 40 °C for 6 h. Corresponding GPC curve is shown in Figure 5b. Profiles (a), (c), (d), and (e) were measured at 25 °C. The arrows show the scattering maxima due to the long period.

(Scheme IV).

To verify the hypothesis concerning the back-biting mechanism described above, we investigated the relationship between the molecular weight of cyclic POM and the crystalline lamella thickness of the original POM obtained under various polymerization conditions.

The lamellar thickness was estimated by the SAX technique. Generally, a semicrystalline polymer gives a scattering maximum at around 10^{-1} nm^{-1} in the scattering vector s ; $s = (2 \sin \theta) / \lambda$ (where θ and λ are half of the scattering angle and the wavelength of the X-ray, respectively). This corresponds to the average repeating interval between crystalline and amorphous regions, the so-called long period. The SAXS profiles measured at 25 °C for POM washed with cleaning solutions and dried under vacuum are shown in Figure 8c,e. These profiles, parts c and e of Figure 8, show no remarkable peak, or even a less-remarkable peak, compared with the corre-

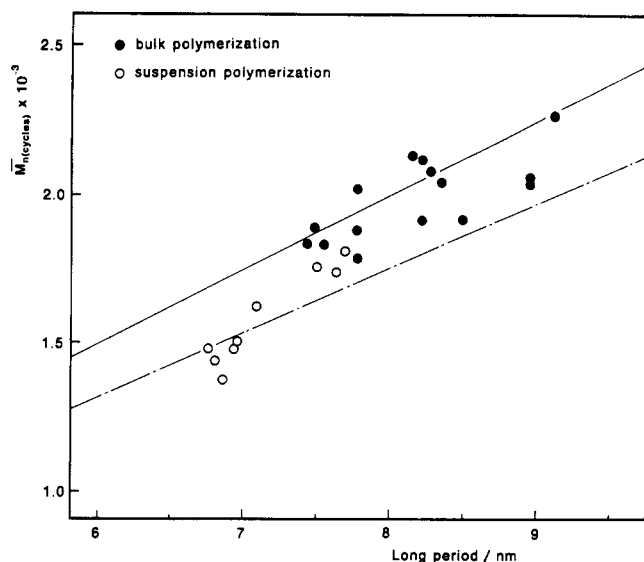


Figure 9. The long period estimate from SAXS desmeared profiles versus \bar{M}_n of macrocycles. The SAXS profiles were obtained by unwashed as-polymerized POM, as shown in parts a and b of Figure 8. $\bar{M}_n(\text{cycles})$ were calculated from GPC curves in the same way as in Figure 1 and Table II. The lines indicate the relationship obtained from eq 1 when ϕ_c is 0.8 (—) and ϕ_c is 0.7 (---).

sponding profiles, parts a and d of Figure 8, respectively, before washing. This is because of the influence of strong zeroth-order scattering from the voids existing in the grain-boundary region of the stacks of POM lamellar crystals. Before washing, the voids were filled by a water-soluble residual monomer and an oligomer which suppressed the zeroth-order scattering and enhanced the scattering maximum from the long period (Figure 8a,b,d). The maximum shifted toward a smaller angle (Figure 8b) upon isothermal annealing of the as-polymerized specimen (Figure 8a) at a temperature (e.g. 100 °C) higher than the reaction temperature (70 °C). This shift is considered to result from lamellar thickening. The peaks in Figure 8a,b,d can evidently be assigned to each long period. However, the actual crystallinity in the grain (i.e., a stack of POM lamella) and the average lamellar thickness could not be determined by the conventional methods, such as densitometry and thermal analysis. Because the quantity of the monomer left in between the grains and within the grains (amorphous regions in a stack of lamella) was unknown, the ratio of the monomer in the grains to that among grains was undetectable.

Figure 9 shows the relation between the long period, calculated by Bragg's equation using SAXS desmeared profiles, and the \bar{M}_n of the lower molecular weight portion (i.e. \bar{M}_n of macrocycles) determined from GPC. The samples were prepared under various suspension and bulk polymerization conditions, where the initial temperature was 70–110 °C and the quantity of $\text{BF}_3 \cdot \text{O}(\text{C}_2\text{H}_5)_2$ used as a catalyst was 9.6×10^{-7} to 9.6×10^{-6} mol. \bar{M}_n of the cyclic POM was limited to the range from 1300 to 2300 and seemed to be proportional to the long period. The stem length of a lamellar crystal (lamellar thickness) was estimated to be 4.2–7.4 nm on the basis of the observed \bar{M}_n , assuming that a back-biting reaction occurs at the nearest chain-folded loops in lamellar crystals. The calculated value of 4.2–7.4 nm is a little smaller than the corresponding long period of 7–9 nm determined experimentally. This result is consistent with the fact that the lamellar thickness must always be smaller than the long period simply because the amorphous region is included. The small PD of the macrocycle may result

from the narrow distribution of the lamellar thickness.

The molecular weight of cyclic POM (M_{cycles}) is related to the lamella thickness (d_c) through a 9_5 -helix of POM crystalline structure as

$$M_{\text{cycles}} = (2d_c/c) \times 9M_u \quad (1)$$

where c is the crystal lattice spacing along the helical axis ($c = 1.73$ nm) and M_u is the formula weight of the repeating unit ($M_u = 30.0$). The lamellar thickness, d_c , the long period, L , and the volume fraction of lamellar crystals in the grain, ϕ_c , are interrelated as $d_c \sim \phi_c L$. Therefore, M_c is proportional to L if ϕ_c is constant. In Figure 9, the relation between M_{cycles} and L is indicated by solid lines on the assumption that ϕ_c is 0.7 or 0.8. The ϕ_c values of 0.7–0.8 agrees with an usual value for the crystallinity of homo-POM.²⁰ The line showing that ϕ_c is 0.7 indicates the proportionality between L and M_c for samples prepared by suspension polymerization; the line showing that ϕ_c is 0.8 indicates the proportionality for samples obtained by bulk polymerization. The proportionality supports the belief that macrocyclic POM with a small PD is caused by a back-biting reaction on the surface of the lamellar crystals.

Conclusion

POM, obtained by cationic polymerizations of TOX, generally has a bimodal molecular weight distribution when polymerization is carried out under conditions where lamellar crystals are deposited simultaneously. The lower molecular weight portion can be isolated from the original POM by alkaline degradation and consists of macrocycles with a narrow molecular weight distribution. The molecular weight of cyclic POM ranges between 1300 and 2300 and is independent of the molecular weight of its original POM. The formation and the narrow molecular weight distribution of the cyclic POM can be explained in terms of an intramolecular transacetalization on the surface of crystalline lamellae. Namely, the length of macrocyclic POM coincides with almost twice the lamellar thickness and the molecular weight of macrocycles changes only with an alteration of the lamellar thickness.

Acknowledgment. We are grateful to Dr. K. Saijo, Kyoto University, for SAXS experiments and Dr. M. Kumakura, Japan Atomic Energy Research Institute, for the experiments using γ -ray. We also thank Prof. K. Saigo, The University of Tokyo, for useful discussions.

References and Notes

- (1) Szymansky, R.; Kubisa, P.; Penczek, S. *Macromolecules* **1983**, *16*, 1000.
- (2) Burg, K. H.; Hermann, H. D.; Rehling, H. *Makromol. Chem.* **1968**, *111*, 181.
- (3) Plesch, P. H.; Westermann, P. H. *J. Polym. Sci., Part C* **1968**, *16*, 3837.
- (4) Jacobson, H.; Stockmayer, W. H. *J. Chem. Phys.* **1950**, *18*, 1600.
- (5) Plesch, P. H. *Pure Appl. Chem.* **1976**, *48*, 287.
- (6) Kubisa, P.; Penczek, S. *Macromol. Chem.* **1979**, *180*, 1821.
- (7) Miki, T.; Higashimura, T.; Okamura, S. *J. Polym. Sci., Polym. Chem. Ed.* **1967**, *5*, 95.
- (8) Miki, T.; Higashimura, T.; Okamura, S. *J. Polym. Sci., Polym. Chem. Ed.* **1967**, *5*, 2977.
- (9) Mateva, R.; Wegner, G.; Lieser, G. *J. Polym. Sci., Polym. Lett. Ed.* **1973**, *11*, 369.
- (10) Wegner, G.; Rodriguez-Baeza, M.; Lucke, A.; Lieser, G. *Makromol. Chem.* **1980**, *181*, 1763.
- (11) Lucke, A. Doctoral Thesis, Freiburg University, 1979.
- (12) Jaacks, V. *Makromol. Chem.* **1966**, *99*, 300.
- (13) Hashimoto, T.; Suehiro, S.; Shibayama, M.; Saijo, K.; Kawai, H. *Polym. J.* **1981**, *13*, 501. Suehiro, S.; Saijo, K.; Ohta, Y.; Hashimoto, T.; Kawai, H. *Anal. Chim. Acta* **1986**, *189*, 41.

- (14) Ishigaki, I.; Morita, Y.; Nishimura, K.; Ito, A. *J. Appl. Polym. Sci.* **1974**, *18*, 1927.
- (15) Collins, G. L.; Greene, R. K.; Berardinelli, F. M.; Garruto, W. V. *J. Polym. Sci., Polym. Lett. Ed.* **1979**, *17*, 667.
- (16) Chien et al. also reported trimodal GPC curves for the ring-opening cationic polymerization of 1,3,6-trioxocane and 2-butyl-1,3,6-trioxocane.²¹ They assumed that the fraction eluted with the smallest retention volume corresponded to the linear high molecular weight polymer and the fractions at higher retention volumes were probably the macrocycles.
- (17) Okamura, S.; Hayashi, K.; Kitanishi, Y. *J. Polym. Sci.* **1962**, *58*, 925.
- (18) This rearrangement, as proposed by the Freiburg group,⁹ makes progress at the Ostwald-Ripening mechanism supported by

- the vaporization-condensation theory of Lifshitz-Slyozov:²² small particles with a high vapor pressure have a tendency to redissolve and depolymerize into the monomer and large particles further grow by a chain-propagation reaction in order to minimize the excess interfacial free energy of the whole system.
- (19) Wunderlich, B. *Fortschr. Hochpolym.-Forsch.* **1968**, *5*, 568.
- (20) *Polymer Handbook*, 2nd ed.; Wiley: New York, 1975; p V-63.
- (21) Xu, B.; Lillya, P.; Chien, J. *Macromolecules* **1987**, *20*, 1445.
- (22) Lifshitz, I. M.; Slyozov, V. V. *J. Phys. Chem. Solids* **1961**, *19*, 35.
- (23) Chen, S. H.; Catherine, E.; Edwards, A. D. *Adv. Chem. Ser.* **1969**, No. 91, 359.

Registry No. POM, 9002-81-7.

Reversible Gelation of Polyoxazoline by Means of Diels-Alder Reaction¹

Yoshiki Chujo, Kazuki Sada, and Takeo Saegusa*

Department of Synthetic Chemistry, Faculty of Engineering, Kyoto University, Yoshida, Sakyo-ku, Kyoto 606, Japan

Received September 5, 1989; Revised Manuscript Received November 28, 1989

ABSTRACT: Polyoxazoline hydrogel was prepared by means of intermolecular Diels-Alder reaction between furan-modified poly(*N*-acetylenimine) (PAEI) and maleimide-modified PAEI, which were synthesized from the partially hydrolyzed PAEIs by the reaction with furan- or maleimidecarboxylic acid, respectively, in the presence of dicyclohexylcarbodiimide. A film was prepared by casting a methanol solution of these two functionalized PAEIs onto a glass slide. After reaction in bulk film in the dark at room temperature for 1 week, the polyoxazoline gel was obtained in a good yield. The film was much swollen in water and stable enough at ambient temperature to be handled. A series of the PAEIs having varying amounts of the functional groups were prepared and subjected to the cross-linking reaction. The swelling degree depended on the content of the functional groups in the prepolymer. These gels were gradually dissolved by heating to regenerate a pair of the starting polymers by the so-called retro-Diels-Alder reaction. This observation shows that the gelation system via Diels-Alder reaction between maleimide moiety and furan moiety in the polymer pendant is thermally reversible. It is the first example of a thermally reversible hydrogel through the covalent bond.

Introduction

Hydrogels are known to be one of the most interesting polymeric materials and have been used in the various fields for several years. The commercially available polymeric hydrogels are usually based on the cross-linked polyelectrolytes such as poly(acrylic acid) salt. A large volume change of the gels with temperature or with solvent has been successfully explained by the phase transition of the cross-linked ionic gel. The generality of these phenomena has been under investigation extensively by Tanaka's group.² In aqueous salts, the swelling degrees of these ionic hydrogels are known to be diminished largely in comparison with those of nonionic hydrogels made from poly(oxyethylene)³ or poly(acrylamide).⁴⁻⁷ However, less varieties of nonionic hydrogels were prepared than those of ionic hydrogels so far.⁸⁻¹³

A thermally reversible hydrogel system prepared from poly(*N*-alkylacrylamide) was also studied for the utilization as a drug delivery system.¹⁴⁻¹⁷ The reversible change of the swelling volume or sol-gel transition with temperature was caused by the change of the physical cross-linking, i.e., the change of the solubility in water. However, very little has been known about the thermally reversible systems through covalent bonds. Only a few examples

were demonstrated by using the thermal equilibrium of Diels-Alder reaction.¹⁸⁻²⁰ However, these covalent cross-linked polymers were studied in view of the polymer processing for thermosetting or thermoplastic properties. Accordingly, they are based on the thermoplastic elastomers such as polyisobutylene¹⁸ or polyphosphazene.²⁰ No study on the thermally reversible cross-linked polymer system through covalent bonds has been carried out using the hydrophilic polymers. This system may offer a thermally reversible hydrogel through the covalent cross-linkings.

We have been studying the ring-opening polymerization of 2-methyl-2-oxazoline (1) for several years.²¹ The resulting poly(*N*-acetylenimine) (PAEI) (polyoxazoline) has high hydrophilicity and high compatibility with several commodity polymers.²² Very recently, we reported the preparation of polyoxazoline gels by two independent methods, i.e., partial hydrolysis cross-linking²³ and copolymerization.²⁴ They have characteristic properties as a nonionic hydrogel, i.e., a large swelling degree both in water and in aqueous salts.

In this article, we describe a novel method for the preparation of polyoxazoline hydrogels by means of Diels-Alder reaction between the maleimide-modified PAEI and